# FY20 LaserNetUS

M. S. Wei

Laboratory for Laser Energetics, University of Rochester

In 2018, the Department of Energy (DOE) Fusion Energy Sciences (FES) within the Office of Science established a network of high-power laser user facilities, LaserNetUS, to invigorate the U.S. high-energy-density (HED) plasma physics and high-field laser community by supporting a new mechanism for scientific discovery and technical innovation. This DOE FES initiative was a direct response to a 2017 report of the National Academy of Sciences that assessed the physics potential in laser-driven high-field science in the U.S., recommending the creation of a broad national network that includes mid-scale laser infrastructure. LaserNetUS started in August 2018 with seven participating mid-scale high-peak-power laser facilities. LLE joined the LaserNetUS in early 2019. In about a year, the network has grown to ten institutions including Colorado State University, Lawrence Berkeley National Laboratory (LBNL), Lawrence Livermore National Laboratory (LLNL), SLAC, The Ohio State University, the University of Michigan, University of Nebraska-Lincoln, Institut National de la Recherche Scientifique, the University of Rochester, and the University of Texas at Austin. Through a coordinated call for proposals and an independent proposal review panel (PRP) process, the LaserNetUS network makes available a variety of ultrafast, high-peak-power and high-energy, petawatt-class lasers including LLE's four-beam high-energy and high-intensity OMEGA EP laser to users who do not have regular access to ultrahigh-intensity lasers.

In its first year of operation, LaserNetUS issued two solicitations for beam time in 2019 and 2020, and awarded beam time for 49 user experiments to researchers from 25 different institutions. As one of the most-requested facilities in the LaserNetUS network, OMEGA EP accepted seven projects (see Table I) with a total of eight shot days for experiments in FY20 and FY21. A total of 70 target shots were successfully conducted for six LaserNetUS projects led by scientists from Johns Hopkins University, LLNL, Princeton Plasma Physics Laboratory (PPPL), Princeton University, and University of California, San Diego (see Table I). FY20 LaserNetUS experiments are summarized below.

***Exploring Novel Target Designs for High-Yield Laser-Created Relativistic Pairs***
Principal Investigator: H. Chen (LLNL)
Co-investigators: S. Kerr and A. Link (LLNL); J. Kim and F. N. Beg (University of California, San Diego); and M. Manuel (General Atomics)

Despite the progress made in the last ten years or so in using lasers to create relativistic electron–positron pair-plasma jets, low pair density has been the key issue preventing the application of laser-produced pairs in laboratory experiments.[1,2] Our prior experimental work[2] showed that while it would be easy to reach orders of magnitude higher pair yield on future lasers that have much higher laser energy and intensities (ex., EP-OPAL), currently the only effective way to increase the positron beam density is to extract more positrons out of solid targets because simulations suggest that only 1% of the positrons created in conventional, solid high-$Z$ targets escape. We have designed two types of novel targets from which the simulation predicts up to a factor-of-10 higher yield. LaserNetUS facility time offered a perfect opportunity for us to test these targets.

A schematic of the target design rationale,[3] together with the target shape for two designs and their respective experimental results, is shown in Fig. 1.

Table I: Seven LaserNetUS projects were awarded beam time on OMEGA EP for target shots in 2019 and 2020. The first six experiments (shaded cells) were successfully conducted during FY20 and the seventh experiment with two approved shot days has been scheduled for FY21.

| Principal Investigator | Lead Institution | Title |
|---|---|---|
| H. Chen | LLNL | Exploring Novel Target Designs for High-Yield Laser-Created Relativistic Pairs |
| T. Duffy | Princeton University | Ultrahigh-Pressure Phase Transition in (Mg,Fe)O: Implications for Exoplanet Structure and Dynamics |
| W. Fox | PPPL | Particle Energization During Magnetic Reconnection in Colliding Magnetized Plasmas on OMEGA EP |
| H. Ji | Princeton University | Plasma Beta Dependence of Particle Acceleration from Magnetically Driven Collisionless Reconnection Using Laser-Powered Capacitor Coils |
| J. Kim | University of California, San Diego | Ion Acceleration from Multipicosecond Short-Pulse Lasers Interacting with Underdense Plasmas |
| Y.-J. Kim | LLNL | Extreme Chemistry of Synthetic Uranus |
| M. P. Valdivia | Johns Hopkins | Electron Density Imaging of Irradiated Foils Through Talbot–Lau X-Ray Deflectometry |

The experimental data showed that although the nested target seemed to alter the positron energy spectrum, no significant enhancement in positron yield was observed on the 10-ps laser pulse, contrary to that in the simulation. Preliminary interpretation is that the resistive magnetic fields are guiding low-energy positrons later in the interaction and/or, the electromagnetic fields are too weak or grow too slowly to collimate early, high-energy positrons. The layer targets showed a trend that matched expectation in positron yield enhancement with a larger number of cavities in the layer targets [Fig. 1(f)]. Here, since positron yield depends on the target material mass with which relativistic electrons interact, the total measured positron numbers were normalized by target (Au) mass. These experimental results demonstrate a part of the effects of self-generated fields inside the target, but a more systematic study with varying cavity gap and numbers will optimize the electron transport and positron generation.[3] Future work includes a detailed understanding of the discrepancy for the nested targets and optimized design for the layer targets to further increase the positron yield.

The team is grateful for the support of LaserNetUS shot time on the OMEGA EP laser. This work was performed under the auspices of the U.S. DOE by LLNL under Contract DE-AC52-07NA27344 and funded by LDRD (17-ERD-010).

***Particle Energization During Magnetic Reconnection in Colliding High-Beta Magnetized Plasmas on OMEGA EP***

Principal Investigators: W. Fox* and A. Bhattacharjee* (PPPL); G. Fiksel and D. B. Schaeffer* (University of Michigan); M. J. Rosenberg (LLE); and K. Germaschewski (University of New Hampshire)
*Also, Princeton University

Understanding the physics of magnetized plasmas is key to unlocking a number of important problems in space and astrophysics. A key feature of explosive processes in astrophysical plasmas is the acceleration of particles to form populations of superthermal, energized particles, such as cosmic rays. Magnetic reconnection is a fundamental mechanism behind these processes, which can explosively release stored magnetic energy, convert it to plasma heat and flows, and accelerate particles.[4,5] Recent experiments using magnetized laser-produced plasmas have opened opportunities to study particle acceleration by magnetic reconnection in the laboratory.[6–8] The experiments collide pairs of plasma plumes that have self-generated strong (~10-T) magnetic fields by the Biermann battery process.[6]

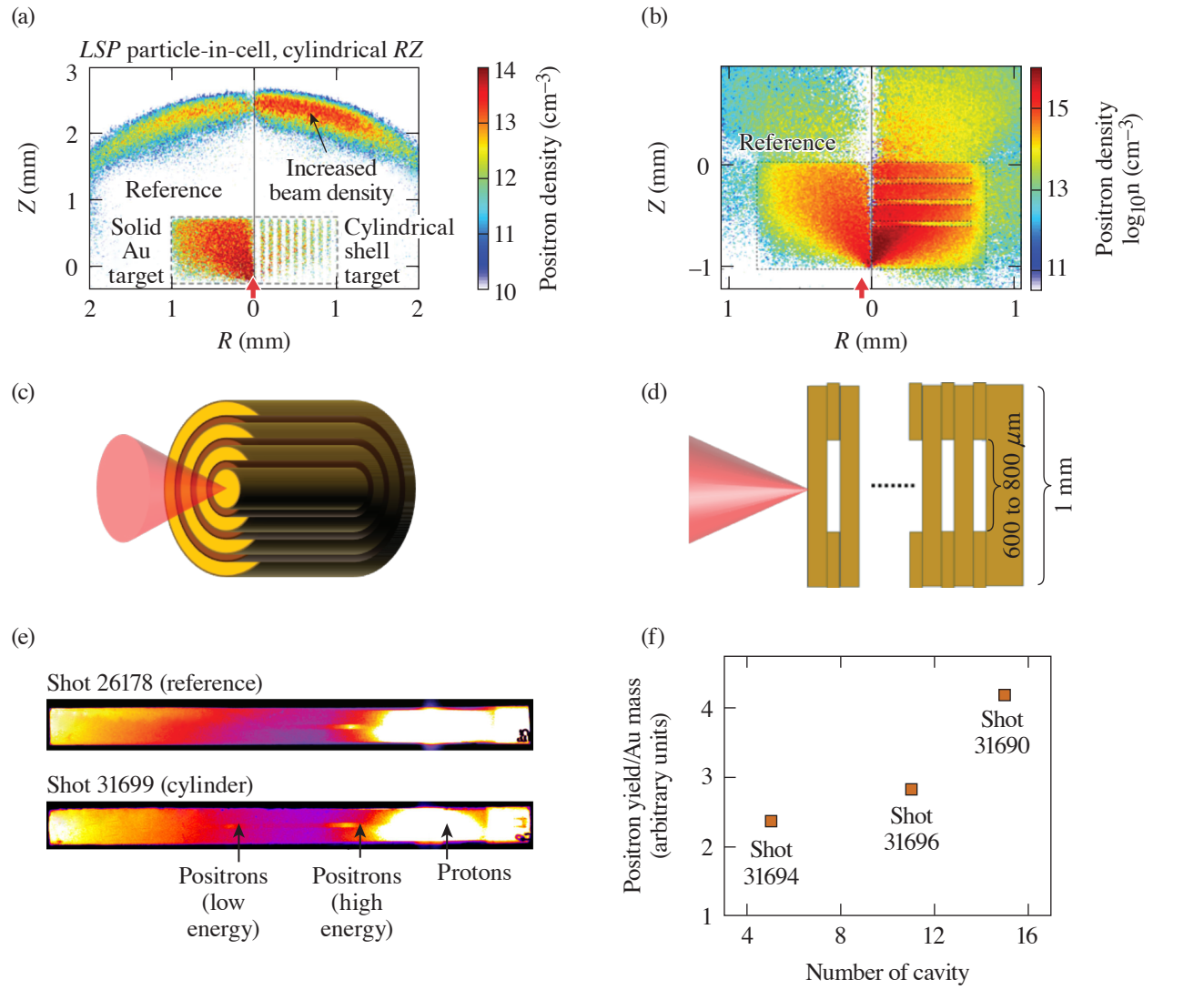


Figure 1
(a) Simulation results for the "nested cylinder target" for positron densities (right) relative to the flat target (left); (b) simulation positron density for the "layer targets" (right) relative to the flat target (left); drawing of the (c) nested target and (d) layer target; experimental results for the (e) nested target and (f) layer target.

We conducted experiments on the OMEGA EP laser to observe the acceleration of high-energy electrons in colliding magnetized plasmas. A key part of this experiment was the confirmation of the results using repeated shots and careful comparison against null experiments. The experimental setup is shown in Fig. 2. A plastic (CH) target is driven by one or two 351-nm laser beams, each focused to a 750-$\mu$m-diam spot. Each beam has an energy of 200 J and a duration of 0.5 ns, which corresponds to a beam power of 0.4 TW and on-target laser intensity of $0.9 \times 10^{14}$ W/cm$^2$. Two types of shots were investigated: reconnection shots and "non-reconnection shots." For reconnection shots, two beams focused 1.6 mm apart were employed. As the plasmas expand, they generate magnetic fields by the Biermann battery effect, and when the plumes collide, it drives reconnection and annihilation of the oppositely directed field. For non-reconnection, or "null" shots, only a single beam was used. Laser parameters were carefully found through experiments to reduce the effects of laser–plasma instabilities (LPI's), such as stimulated Raman scattering (SRS) or two-plasmon decay, which can also accelerate particles. Fast particles were observed using a single-channel electron spectrometer (SC-ESM).

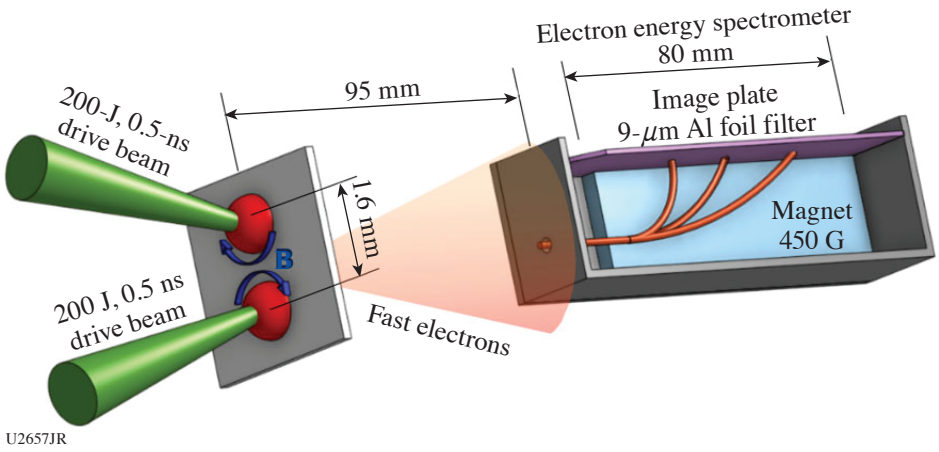


Figure 2
Experimental setup. A plastic (CH) target is driven by one or two 351-nm laser beams focused to a 750-$\mu$m-diam spot. Each beam has an energy of 200 J and a duration of 0.5 ns. The fast electrons were observed by a magnetic energy spectrometer placed 95 mm from the target. The electrons entering the spectrometer through a 0.7-mm pinhole collimator are dispersed by a permanent magnetic field of 450 G and registered by an image plate placed on top of the magnets. Several electron trajectories corresponding to different energies are sketched.

Figure 3 shows a spectrum of the observed particles, comparing a single-plume null experiment with double-plume merging experiments. The non-reconnection data are expressed as a sum over two shots that individually shot the two drive beams from the double-plume experiment. This is important since the levels of energized particles are found to naturally vary between the drive beams. Somewhat surprisingly, energized particles are observed even for null experiments; this likely indicates a residual level of LPI, even though the scattered light from the LPI was below the detection limit on the full-aperture backscatter station (FABS) diagnostics. However, the two-beam reconnection experiments show a significant enhancement of the energized particles beyond the null experiment. This is reproduced over multiple beam pairs, with the error bars shown as the shaded regions. The spectra have approximately exponential profiles where the effective energetic electron temperature increases from 18 keV to 29 keV from non-reconnection to reconnection shots, an increase by a factor of 1.6.

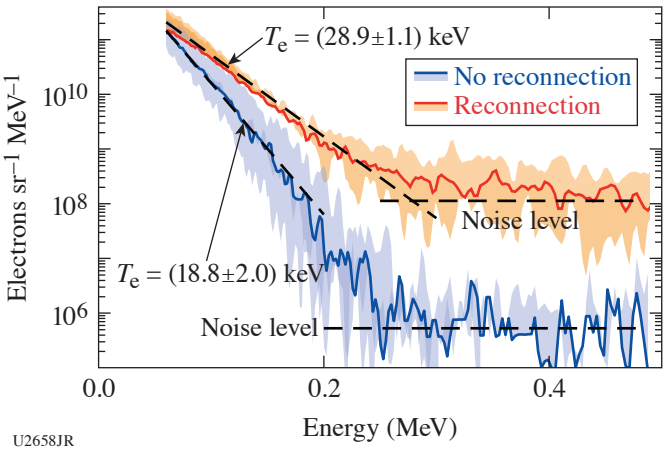


Figure 3
Electron energy spectra for reconnection (red) and non-reconnection (blue) shots. The null, non-reconnection results are summed over both drive beams, shot individually.

These results therefore have carefully shown the enhancement of energized particles in merging magnetized plasmas. Comparison of the experimental data with theory and models of particle acceleration[7,8] is underway, including processes such as direct acceleration by the strong electric fields associated with reconnection, Fermi-type processes in regions of contracting magnetic fields, and betatron energization in regions where fields rapidly compress.

This material is based upon work supported by the Department of Energy National Nuclear Security Administration under Award Number DE-NA0003856, the University of Rochester, and the New York State Energy Research and Development Authority.

***Magnetic Reconnection at Low-Beta Plasmas in Laser-Driven Capacitor Coil Experiment***

Principal Investigators: H. Ji, S. Zhang, A. Chien, and L. Gao (Princeton University); E. Blackman (Department of Physics and Astronomy, University of Rochester), P. M. Nilson (LLE); G. Fiksel (University of Michigan); and H. Chen (LLNL)

Magnetic reconnection is a ubiquitous astrophysical phenomenon at low-$\beta$ plasmas that rapidly converts magnetic energy into plasma flow energy, thermal energy, and nonthermal energetic particles. The nonthermal particles are often an observational signature of magnetic reconnection since it is considered an efficient acceleration mechanism in astrophysical and space plasmas. The diagnosis of the reconnection-accelerated nonthermal particles was limited, however, in magnetically driven devices due to the relatively small mean free path compared with the system size. To overcome this limitation, we have developed a platform using laser-driven capacitor coils, creating a magnetized plasma with low $\beta$ similar to the astrophysical conditions. In this platform, the reconnection-accelerated electrons can escape the mm-scale plasma and be diagnosed by spectrometers.

In FY20, to study the particle acceleration in the magnetic reconnection at low-$\beta$ plasmas, we performed one day of experiments on OMEGA EP under the support of the LaserNetUS program. As shown in Fig. 4(a), two 1-ns, 1.25-kJ UV beams irradiate the capacitor's backplate, producing hot electrons via laser–plasma instabilities. When these hot electrons escape, they create 10s to ~100-kV high voltages driving an ~56-kA peak current in the coils.[9] This current can generate an ~90-T magnetic field in the coil center and ~30 T in the reconnection region. The magnetic field and the magnetic reconnection features were diagnosed in the previous experiments.[9,10]

To diagnose the accelerated electrons, we used Osaka University's electron spectrometer (OU-ESM) and two SC-ESM's placed in different directions. As shown in Fig. 4(b), the channel 5 of OU-ESM facing the front of the target captured the 20- to 70-keV electrons accelerated by the electric field in the reconnection. The SC-ESM facing the back of the target captured lower-temperature spectra in the reconnection experiments than in the reference experiment, indicating particle deceleration due to the electric field. The measured electron spectra and the angular dependence will be compared with the particle-in-cell simulations.

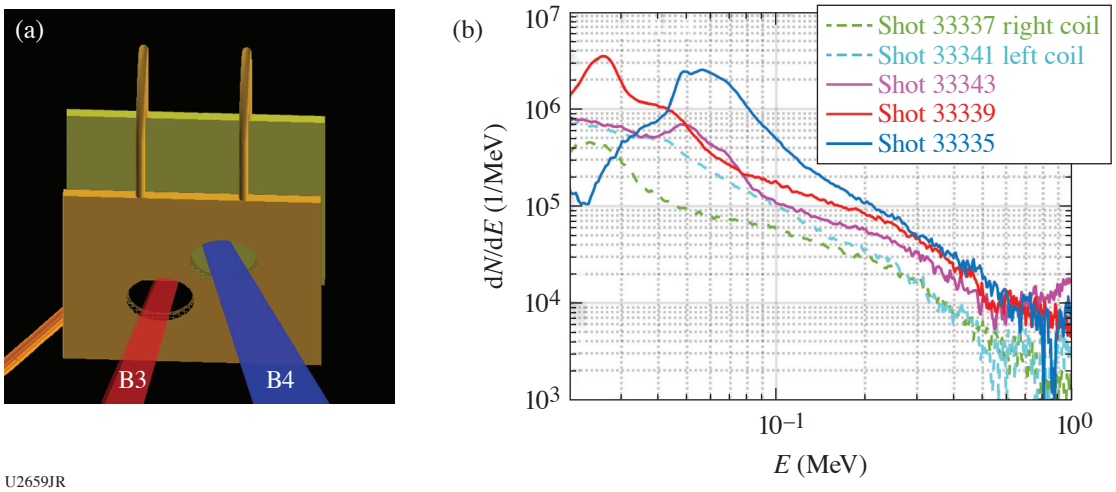


Figure 4
(a) OU-ESM channel 5 view in the reconnection experiment with UV lasers irradiating the capacitor coil target. (b) The OU-ESM-measured electron spectra. Dashed lines are from two reference experiments that used a target with one coil. The solid lines are from reconnection experiments using two-coil targets. Accelerated electrons around 20 keV to 70 keV are seen in the reconnection experiments.

During this shot day, besides the particle acceleration measurement, we tested a new platform that uses a short-pulse IR laser to drive a capacitor-coil target. We varied the IR pulse duration and energy to study the magnetic field's dependence on the laser parameters. As shown in the proton radiography images (Fig. 5), even though the 0.7-ps, 300-J laser has a 20× higher intensity than the 15-ps, 300-J laser, the magnetic field generated by the 0.7-ps laser is ~40% lower than that driven by the 15-ps laser. This pulse-duration dependence will aid in validating our lump-circuit model.

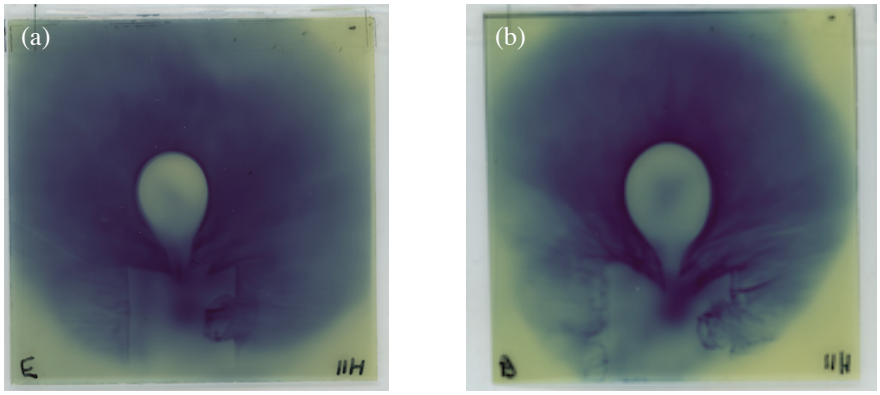


U2660JR

Figure 5
Comparison of the proton radiography images between (a) the capacitor coil driven by a 0.7-ps, 300-J laser and (b) the capacitor coil driven by a 15-ps laser. The void diameter in the 0.7-ps laser experiment is 20% smaller than that in the 15-ps experiment, which indicates an ~40% lower current and magnetic field.

This material is based upon work supported by DOE Office of Science, Fusion Energy Sciences under Contract No. DE-SC0020005: the LaserNetUS initiative at the Omega Laser Facility and under Contract No. DE-SC0020103 (HEDLP).

***High-Energy Protons from OMEGA EP Multipicosecond Pulses Using Submicron Targets***

Principal Investigators: J. Kim, C. McGuffey, K. Bhutwala, and F. N. Beg (University of California, San Diego); G. Cochran, T. Ma, D. Mariscal, G. G. Scott, and S. Wilks (LLNL); S. R. Klein (University of Michigan); and R. Simpson (MIT)

We have investigated the acceleration of protons and ions using the OMEGA EP short-pulse laser with submicron-thick targets while exploring the pulse duration. Ion acceleration driven by short-pulse lasers has been an active research area in high-energy-density physics because it is appealing for its potential broad range of applications including neutron sources, exotic isotope creation, novel inertial confinement fusion (ICF) ignition schemes, proton probing, and ion therapy.

For two decades, numerous acceleration mechanisms, leading to tens of MeV/nucleon ion acceleration, have been described in simulations and reported experimentally, many of which benefit from a submicron target or even rely on the target becoming transparent before or during the main pulse interaction. Laser prepulse—light that precedes the main pulse—sets the conditions of the target interaction and is thought to have thwarted many attempts to pass the 58-MeV mark set in 1999.[11] With the well-characterized OMEGA EP prepulse[12] and ongoing work into a plasma mirror configuration that would further reduce prepulse energy, it is an excellent time to re-evaluate the ion acceleration performance that can be achieved.

Furthermore, recent findings have shown promise in using multipicosecond laser pulse duration for increasing the maximum proton energy, in spite of conventional wisdom that higher intensity is always better. It has been predicted through simulations by our group[13] and shown in recent experiments on the National Ignition Facility (NIF) Advanced Radiographic Capability (ARC) laser[14] that 1- to 10-ps lasers outperform subpicosecond lasers in terms of proton energy for mildly relativistic intensities. In those works, we showed that multipicosecond pulse duration leads to a time-evolving (increasing) temperature of the hot electrons being directed into the target that in turn accelerates protons longer and to higher maximum energy. We also hypothesized, before this project, that multipicosecond pulses would provide synergistic effects in combination with submicron targets due to the higher likelihood of transparency during the main pulse.

During a recent OMEGA EP shot day, we measured proton beams from the short-pulse beams with laser durations from 0.7 to 10 ps and targets of parylene (CH) or aluminum with thickness from 100 nm to 3 $\mu$m. We also fielded a special target consisting of two 100-nm CH foils separated by 300 $\mu$m to test the concept of a fast shutter. The primary diagnostic was a stack of radiochromic films and filters designed to have a proton punch-through energy of 70 MeV for the last layer. The target was rotated to a 10° angle of incidence such that the target normal and laser propagation directions could be distinguished on the films.

For a control shot using the best compressed-pulse duration (nominally 0.7 ps) and 3-$\mu$m-thick parylene, protons reached the $45^{+}$-MeV film layer but not the $58^{+}$-MeV layer, an unsurprising result. However, all the shots with 2- to 3-ps duration and full energy produced a signal all the way to the last layer of the film ($70^{+}$ MeV). Figure 6 shows the last layer of film for three targets, with the 300 nm of CH producing the strongest signal on that layer. We believe these are the most energetic protons measured from the facility to date, and the result begs for the design of a film holder to accommodate higher energy.

We are investigating other interesting results from the shot day including 4$\omega$ probe images that may inform us about transparency of the different targets. An example interferogram is shown in Fig. 7 for the shot with the fast shutter test target (2 × 100 nm of CH). The interferogram shows plasma in line with the laser axis on the front and back layers of both foils, suggesting that the front foil became transparent during or before the main pulse.

This material is based upon work supported by the Department of Energy Fusion Energy Sciences LaserNetUS.

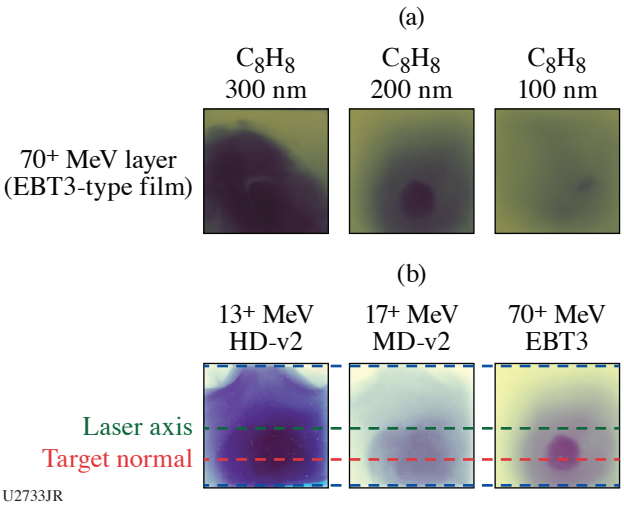


Figure 6
(a) The last layer of a radiochromic film stack, corresponding to 70-MeV proton energy, is shown for three target thicknesses and fixed laser conditions: 500 J in 2 ps. (b) The beam profile and directionality can be seen in three select layers of a single shot.

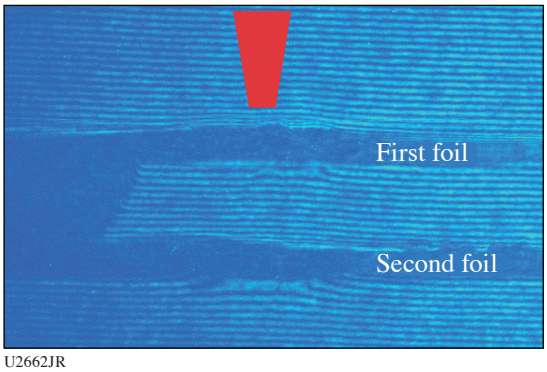


Figure 7
Interferogram from the 4$\omega$ probe side-on to a double-foil target. Plasma, indicated by bent fringes, is apparent on both sides of both targets at the probing time, 30 ps after the 3-ps main pulse arrives from the top of the image. This suggests the 100-nm parylene became transparent before the end of the main pulse.

***High-Pressure Polymorphism of ZnO Under Laser-Driven Ramp Compression***

Principal Investigators: I. K. Ocampo, D. Kim, and T. S. Duffy (Department of Geosciences, Princeton University); and F. Coppari and R. F. Smith (LLNL)

A goal of the XRDEOSEP Campaign was to investigate the phase diagram of ZnO, a wide-bandgap semi-conductor (3.37 eV) well suited for use in electronic and optoelectronic devices.[15] There has long been interest in high-pressure polymorphism in ZnO from both theory and experiment as a test case for the B1–B2 phase transition. Static compression experiments have shown that under relatively low pressures (~10 GPa), ZnO undergoes a phase transition from a wurtzite-type structure ($P6_3mc$) to a B1-type structure ($Fm\text{-}3m$).[16] No further phase transitions have been observed in ZnO experimentally up to ~209 GPa, but density functional theory calculations predict that the B2 phase ($Pm\text{–}3m$) will become stable at high pressures.[17,18] The calculated B1–B2 transition pressures vary considerably from one study to another (243.5 to 316 GPa). By combining the unique pulse-shaping capabilities of OMEGA EP with nanosecond x-ray diffraction, we sought to observe the crystal structure of ZnO across the predicted B1–B2 transition. Furthermore, constraining the transition pressures and equations of state for ZnO allows us to test the efficacy of the theoretical calculations.

ZnO powders were compressed in a short piston diamond anvil cell with 800-$\mu$m culets to ~1.7 GPa, resulting in ~10-$\mu$m-thick foils. These foils were sandwiched between a single-crystal diamond ablator and a LiF window. A 10-ns ramp-shaped pulse was used to ablate the surface of the target sandwich and quasi-isentropically compress the sample. When the target was at approximately peak stress, a 1-ns, 500-J laser pulse was used to irradiate a Cu backlighter foil, generating quasi-monochromatic x rays that were diffracted and recorded using the powder x-ray diffraction image plate (PXRDIP) diagnostic. The active shock breakout diagnostic monitored the particle velocity at the ZnO–LiF interface, which was then used to infer the stress history in the sample.

We conducted four experiments and collected high-quality diffraction data from 253 to 448 GPa. At 253 GPa, four reflections from the sample were observed, all corresponding to the B1 phase. Two intermediate stress experiments (351 and 396 GPa) show diffraction from the B1 phase as well as the B2-type structure (Fig. 8). This is the first experimental observation of the post-B1 phase in ZnO. At our highest achieved stress (448 GPa), diffraction from the B1 phase is still observed but is highly textured. Under the nanosecond time scales of these experiments, ZnO exhibits a wide B1–B2 mixed phase region (~100 GPa). This work is ongoing and further experiments will be conducted to better constrain the EOS of the B2 phase.

This work was supported by DOE Office of Science, Fusion Energy Sciences under Contract No. DE-SC0020005: the LaserNetUS initiative at the Omega Laser Facility.

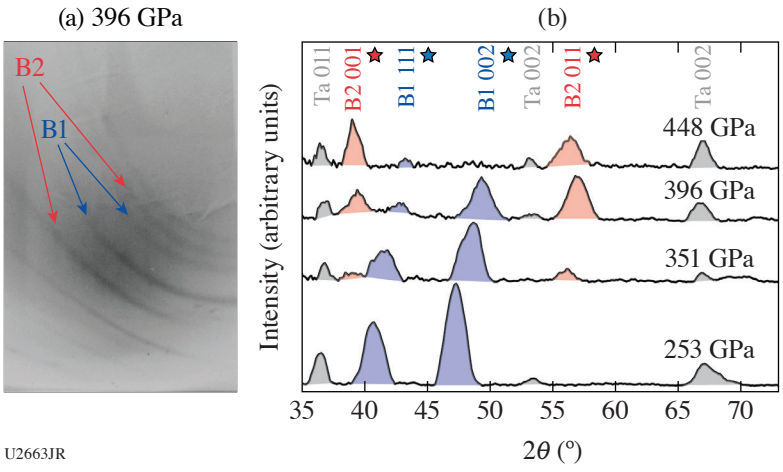


Figure 8
(a) Recorded raw diffraction data from shot 32575. Red arrows highlight the presence of reflections corresponding to the high-pressure phase (B2 type), whereas the blue arrows indicate diffraction from the low-pressure phase (B1 type). (b) Integrated diffraction patterns display the two highest-intensity peaks from both the B1 and B2 structures. Only the B1 phase is observed in the lowest stress experiment, whereas the B1 and B2 phases are observed in all other experiments.

***Talbot–Lau X-Ray Deflectometry (TXD) Electron Density Diagnostic in Laser–Target Interactions***

Principal Investigators: M. P. Valdivia, D. Stutman, and M. Schneider (Physics and Astronomy Department, Johns Hopkins University)

X-ray refraction-based imaging diagnostics for high-energy-density laboratory plasmas have been developed by the Johns Hopkins University X-ray Imaging and Plasma Spectroscopy group. Experiments have been conducted at LLE to benchmark a Talbot–Lau[19–21] x-ray deflectometer for the OMEGA EP laser (EP-TXD).[22] The imaging diagnostic uses standard laser-based x-ray backlighters to directly measure electron density gradients and can simultaneously measure refraction, attenuation, elemental composition, and small-angle scatter.[23] Differential phase-contrast imaging offers a stronger contrast mechanism since refraction signatures are much larger than attenuation when probing low-$Z$ matter with 1- to 100-keV x rays.[24] For this reason, x-ray refraction imaging techniques based on Talbot–Lau interferometry have been developed to characterize fusion-relevant dense plasmas. The EP-TXD rail detects x-ray refraction angles caused by refraction index changes within an object placed along its line of sight.[25,26] This angle ($\alpha$) is proportional to the probed object electron density gradient, enabling 2-D electron density mapping through moiré imaging by following

$$a(x,y) = \lambda / 2\pi \Delta\Phi(x,y), \tag{1}$$

where $\lambda$ is the probing x-ray beam wavelength and $\Phi$ is the phase. In the deflectometry configuration, one fringe shift is equivalent to the system's effective angular sensitivity. From Eq. (1), considering a critical density of $n_c = 4.56 \times 10^{28}$ cm$^{-3}$ at 8 keV, the EP-TXD platform can measure electron densities of $\sim 10^{23}$ to $10^{24}$ cm$^{-3}$.

Sponsored by the National Laser Users Facility grant, the EP-TXD diagnostic platform has been established in collaboration with researchers at LLE. An experimental platform was designed to probe the ablation front of an irradiated foil to obtain electron density through TXD. Electron density mapping above $10^{23}$ cm$^{-3}$ will help benchmark standard magnetohydrodynamic (MHD) codes that fail to accurately model ablating plasma properties. The results obtained can help validate codes in the longstanding problem of ablation dynamics in laser-produced coronal plasmas and aid in two-plasmon decay and general laser–plasma interaction studies, for example.[27,28]

Preliminary experiments were performed using the Multi-Terawatt laser to evaluate x-ray backlighter source spectra quality, size, and flux. Detector performance was also studied in context of moiré fringe contrast and spatial resolution in order to optimize TXD diagnostic capabilities.[29] These experiments established backlighter target, detector, and laser parameters for a new Irradiated Foil LaserNetUS Campaign on OMEGA EP, where an x-ray backlighter evaluation was performed followed by ablation profile imaging. Driving beam laser parameters were adjusted, in similarity to x-ray backlighter target and laser parameters, to obtain a moiré image of the ablation profile with a measured spatial resolution <10 $\mu$m. The experiment imaged—for the first time—plasma targets using laser-produced x-ray backlighters.

A refraction-angle map [Fig. 9(c)] was retrieved from recorded fringe shifts [Fig. 9(b)], showing that x-ray phase contrast can diagnose high-energy-density physics (HEDP) experiments through x-ray refraction imaging. Figure 9(b) also shows a highly dense ablation front close to the foil target (left side), well above the $10^{25}$ cm$^{-3}$ detection limit of EP-TXD. TXD was successfully implemented on OMEGA EP, demonstrating it can obtain moiré images with high x-ray refraction angle sensitivity and spatial resolution. Moiré deflectometry will allow us to accurately measure density gradients in HED plasmas with high spatial resolution. Further analysis and measurements are underway as well as the extension of TXD diagnostic capabilities through monochromatic x-ray backlighting.

This material is based on work supported by DoE NNSA under Award Number DE-NA0003882 and DE-NA0003941. DOE Office of Science FES: DE-SC0020005 LaserNetUS at the Omega Laser Facility.

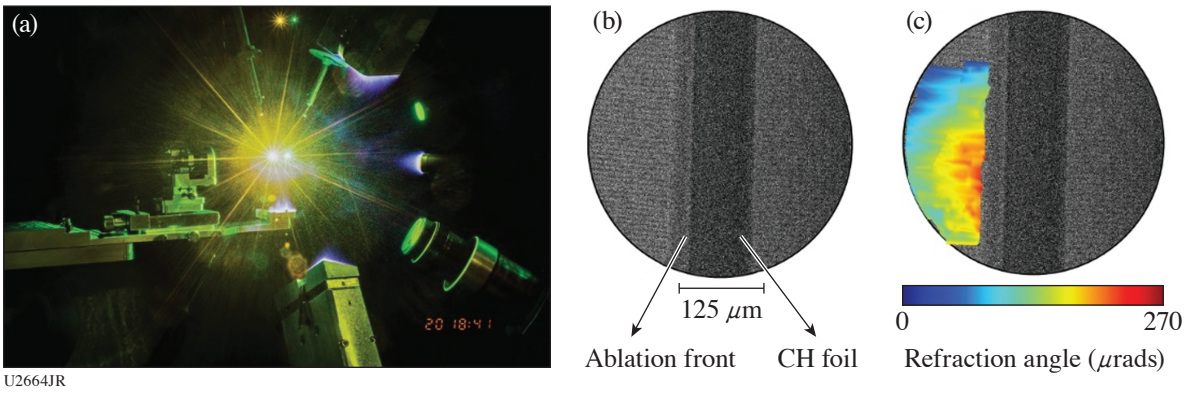


Figure 9
(a) Visible camera image of the EP-TXD diagnostic in the Irradiated Foil Campaign. (b) Raw moiré image of the 125-$\mu$m CH irradiated foil (150 J, 1 ns) obtained through TXD at 5 ns. (c) Refraction-angle 2-D map retrieved through TXD methods.

REFERENCES

1. H. Chen *et al.*, Phys. Plasmas **22**, 056705 (2015).
2. H. Chen *et al.*, Phys. Rev. Lett. **114**, 215001 (2015).
3. J. Kim *et al.*, "Efficient Positron Generation by Control of Laser-Driven Electrons in Novel Targets," to be submitted to Physics of Plasmas.
4. M. Yamada, R. M. Kulsrud, and H. Ji, Rev. Mod. Phys. **82**, 603 (2010).
5. J. F. Drake *et al.*, Nature **443**, 553 (2006).
6. M. J. Rosenberg *et al.*, Phys. Rev. Lett. **114**, 205004 (2015).
7. W. Fox *et al.*, Phys. Plasmas **24**, 092901 (2017).
8. S. R. Totorica, T. Abel, and F. Fiuza, Phys. Rev. Lett. **116**, 095003 (2016).
9. A. Chien *et al.*, Phys. Plasmas **26**, 062113 (2019).
10. L. Gao *et al.*, Phys. Plasmas **23**, 043106 (2016).
11. R. A. Snavely *et al.*, Phys. Rev. Lett. **85**, 2945 (2000).
12. C. Dorrer, A. Consentino, and D. Irwin, Appl. Phys. B **122**, 156 (2016).
13. J. Kim *et al.*, Phys. Plasmas **25**, 083109 (2018).
14. D. Mariscal *et al.*, Phys. Plasmas **26**, 043110 (2019).
15. X. Sha *et al.*, Sci. Rep. **5**, 11003 (2015).

16. H. Liu, J. S. Tse, and H. Mao, J. Appl. Phys. **100**, 093509 (2006).

17. J. E. Jaffe *et al.*, Phys. Rev. B **62**, 1660 (2000).

18. Z. Li *et al.*, Phys. Rev. B **79**, 193201 (2009).

19. H. F. Talbot, Lond. & Edin. Phil. Mag. & J. of Sci., Third Series **9**, 401 (1836).

20. A. Momose *et al.*, Jpn. J. Appl. Phys. **42**, L866 (2003).

21. F. Pfeiffer *et al.*, Nat. Phys. **2**, 258 (2006).

22. M. P. Valdivia *et al.*, Rev. Sci. Instrum. **91**, 023511 (2020).

23. N. Bevins *et al.*, Med. Phys. **39**, 424 (2012).

24. D. Stutman and M. Finkenthal, Rev. Sci. Instrum. **82**, 113508 (2011).

25. M. P. Valdivia, D. Stutman, and M. Finkenthal, Rev. Sci. Instrum. **85**, 073702 (2014).

26. M. P. Valdivia *et al.*, Rev. Sci. Instrum. **87**, 11D501 (2016).

27. J. R. Fein *et al.*, Phys. Plasmas **24**, 032707 (2017).

28. R. P. Drake *et al.*, Phys. Fluids B **1**, 1089 (1989).

29. M. P. Valdivia *et al.*, Rev. Sci. Instrum. **89**, 10G127 (2018).